



## Multiphase transient analysis of horizontal wells during CO<sub>2</sub>-EOR

Longlong Li<sup>a,b,\*</sup>, Minglu Wu<sup>c</sup>, Yuewu Liu<sup>a,d</sup>, Jiuge Ding<sup>a</sup>, Ahmad Abushaikha<sup>b</sup>

<sup>a</sup> Institute of Mechanics, Chinese Academy of Sciences, Beijing, China

<sup>b</sup> College of Science and Engineering, Hamad Bin Khalifa University, Education City, Qatar Foundation, Doha, Qatar

<sup>c</sup> Key Laboratory of Unconventional Oil & Gas Development, China University of Petroleum (East China), Ministry of Education, Qingdao, China

<sup>d</sup> University of Chinese Academy of Sciences, Beijing, China

### ARTICLE INFO

#### Keywords:

Horizontal well

CO<sub>2</sub>-EOR

Pressure transient analysis

Miscibility

Corresponding analysis

### ABSTRACT

We apply a numerical well test model that considers the transient flow in well and the complex displacement mechanisms for the multiphase transient analysis of horizontal wells during CO<sub>2</sub>-EOR. Aimed to perform a systematic and reliable analysis, we run the model on a high-resolution non-uniform grid to accurately capture the transient flow in the near wellbore region as well as the complex displacement process. In this work, we interpret the pressure response curve in two steps to find the root causes of the particular transient behaviors. First, we identify five typical flow regimes through the traditional pressure transient analysis method for horizontal wells which gives us a basic understanding of the characteristics of the pressure response curve. Second, assisted with the corresponding analysis method, we figure out the durations on the curve that correspond to different component banks. By taking the complex displacement mechanisms into consideration, we find that the component banks have a large influence on the curve and identify the root cause of each unique characteristic. Besides, we conduct a systematic sensitivity analysis with respect to multiple parameters such as miscible condition, wellbore storage coefficient, skin factor, horizontal well length, anisotropy, and amount of injected CO<sub>2</sub>. Finally, we have a better understanding of the transient pressure behavior of horizontal wells during CO<sub>2</sub>-EOR, find a way to determine the miscibility underground, and feel more confident in applying the pressure transient data for analysis and parameter estimation.

### 1. Introduction

As proven in multiple field applications (Malik and Islam, 2000; Ghahfarokhi et al., 2016; Hosseini-noosheri et al., 2018; Choi et al., 2013; Zhang et al., 2015) and research work (Orr and Taber, 1984; Sun et al., 2013; Altundas et al., 2017; Rogmo et al., 2019, 2020; Massarweh and Abushaikha, 2021; Wang et al., 2021), the CO<sub>2</sub>-EOR technology holds great potentials to drastically enhance the oil recovery for subsurface reservoirs. Meanwhile, arisen with an urgent demand for mitigating the greenhouse effect (Schneider, 1989; Nordhaus, 1991), it becomes more and more attractive because of its environmentally friendly way to store the CO<sub>2</sub> in a depleted oil/gas reservoir. In field applications, the performance of this technology is mainly evaluated by two indicators including the development of miscibility and gas breakthrough time. Owing to the obvious contrast between the viscosities of oil and gas as well as the density, the factors such as the reservoir condition, heterogeneity, and the composition of hydrocarbons both have a great influence on the two indicators. Thus, the selection of an optimal

development strategy in CO<sub>2</sub>-EOR is more important than that in other EOR technologies. As discussed in (Bagci, (2007)), the horizontal injection well displays many advantages when compares with the vertical wells. For example, it helps to gain high injectivity, a delayed breakthrough of the injected CO<sub>2</sub>, and pressure maintenance that is quite important for the development of miscibility. However, the viscous fingering and gravity override (Moortgat, 2016; Lyu et al., 2021; Tchelepi et al., 1993) that are mainly controlled by the viscosity and density contrasts between oil and gas phases are still a concern as well as the conventional patterns using vertical wells. Continuous monitoring of the displacement process is quite necessary for a horizontal well during CO<sub>2</sub>-EOR.

Currently, there are three methods to monitor the displacement process: the seismic approach (Kendall et al., 2003; Araman et al., 2008; Terrell et al., 2002), the mass balance equations (Tian and Zhao, 2008), and the pressure transient analysis (MacAllister, 1987; Tang and Ambastha, 1988; Su et al., 2015; Li et al., 2016, 2018). Having accurate measurement and easy operation, the third one shows more prospects

\* Corresponding author. Institute of Mechanics, Chinese Academy of Sciences, Beijing, China.

E-mail address: [lilonglong.upc@gmail.com](mailto:lilonglong.upc@gmail.com) (L. Li).

<https://doi.org/10.1016/j.petrol.2021.109895>

Received 25 August 2021; Received in revised form 21 October 2021; Accepted 21 November 2021

Available online 26 November 2021

0920-4105/© 2021 Elsevier B.V. All rights reserved.

than the previous two methods which are expensive in operation and simplified a lot in assumption respectively. However, constrained by the interpretation method, it is still challenging to take full use of the transient data, especially for horizontal injection wells. In 1987, MacAllister (1987) proposed a three-region composite analytical model for a vertical injection well. Then, Tang et al. (Tang and Ambastha, 1988) and Su et al. (2015) made some investigations following this conception. The simplifications in the CO<sub>2</sub> displacement process make it difficult to reproduce the transient pressure accurately. To overcome the drawbacks, Li et al. (2016) proposed a numerical well test model based on the compositional model that can fully consider the complex mechanisms of CO<sub>2</sub> flooding. Followed by this work, Li et al. (2018) included the multi-segment well model into the numerical well test model and proposed a corresponding analysis method to interpret the characteristics of the well test curve in detail. Generally, the work is limited to vertical wells. An investigation into the pressure transient analysis of horizontal wells during CO<sub>2</sub>-EOR is quite necessary.

Regarding the well test theory of horizontal wells, researchers have already proposed many well test models and made meaningful investigations. Clonts and Ramey (1986) proposed analytical equations for two flow regimes including short-time radial flow and long-time pseudo-radial flow. Daviau et al. (1988) proposed analytical solutions for the two flow regimes with consideration of the wellbore storage effect. Goode and Thambynayagam (1987) proposed an analytical solution for the pressure drawdown and buildup and identified four flow regimes including early-time radial flow, intermediate-time linear flow, late-intermediate-time radial flow, and late-time linear flow. Derived from the previous work, many detailed investigations (Ozkan et al., 1989; Odeh and Babu, 1989; Rosa and Carvalho, 1989; Kuchuk et al., 1991; Kuchuk, 1995; Cheng, 2003) were conducted by considering multiple boundary conditions. Moreover, Yao and Wu (2011) proposed a numerical well test model using the streamline method which can consider a multiphase flow in real geological models. Again, a well test theory of horizontal CO<sub>2</sub> injection wells is quite needed since the above work is not applicable in CO<sub>2</sub>-EOR.

In this work, we apply a numerical well test model for the multiphase transient analysis of horizontal wells during CO<sub>2</sub>-EOR. Different from the previous horizontal well models, the EoS based compositional model is employed to consider the complex displacement mechanisms. Moreover, we implement the numerical well test model that also considers the transient flow in well with the wellbore storage model in a fully-implicit parallel reservoir simulator (Li and Abushaikha, 2019, 2020, 2021; Li et al., 2020). In this way, we can run simulations on a high-resolution non-uniform grid to accurately capture the transient behaviors. Then, we present a new approach that interprets the pressure response curve in two steps to complete a root cause analysis of the particular transient behaviors. First, we identify five flow regimes on the log-log plot of pressure and pressure derivative curves using the traditional pressure transient analysis method. Benefit from that, we have a basic understanding of the characteristics of the pressure response curve from a horizontal CO<sub>2</sub> injection well. Second, we analyze the effect of component banks, which are induced by the complex mechanisms of CO<sub>2</sub> flooding and make the curves different from those of traditional horizontal well models, on the curves through the corresponding analysis method (Li et al., 2018). Taking the phase behavior of each bank into interpretation, we have a further understanding of the transient pressure behavior and find the root cause of the unique characteristics. Besides, we conduct a systematic analysis of the pressure transient data by investigating the sensitivity of the curves to miscible condition, wellbore storage coefficient, skin factor, horizontal well length, anisotropy, and amount of injected CO<sub>2</sub>. The systematic work in this paper provides theoretical and technical support for the pressure transient analysis of a horizontal CO<sub>2</sub> injection well and points out a reliable way to monitor the CO<sub>2</sub> displacement process in horizontal well patterns.

## 2. Mathematical model

In this work, for the purpose of capturing the transient effects during CO<sub>2</sub>-EOR accurately, we implement a numerical well test model that couples the wellbore storage model and EoS based compositional model in a fully-implicit parallel reservoir simulator (Li and Abushaikha, 2019, 2020, 2021; Li et al., 2020).

### 2.1. Conservation equations

Assuming  $n_c$  hydrocarbon components in oil and gas phases underground, the transport equations can be written as follows:

$$\frac{\partial}{\partial t} \left( \phi \sum_{j=1}^{n_p} x_{cj} \rho_j S_j \right) + \text{div} \sum_{j=1}^{n_p} x_{cj} \rho_j \mathbf{v}_j + \sum_{j=1}^{n_p} x_{cj} \rho_j \tilde{q}_j = 0, \quad c = 1, \dots, n_c. \quad (1)$$

Where  $t$  is the time;  $\phi$  is the reservoir porosity;  $n_p$  is the number of phases;  $x_{cj}$  is the mole fraction of component  $c$  in phase  $j$ ;  $\rho$  is the phase density;  $S$  is the saturation;  $\tilde{q}_j$  is the phase rate per unit volume;  $n_c$  is the number of components; the Darcy velocity of phase  $j$  without considering the capillary pressure is:

$$\mathbf{v}_j = - \mathbf{K} \frac{k_{rj}}{\mu_j} \nabla P, \quad (2)$$

where  $\mathbf{K}$  is the permeability in tensor format;  $\mu$  is the viscosity that is evaluated by Lohrenz-Bray-Clark (LBC) correlation (Lohrenz et al., 1964);  $P$  is the pressure;  $k_{rj}$  is the relative permeability of phase  $j$  which is calculated as follows:

$$k_{rj} = F_k k_{rj}^{imm} + (1 - F_k) k_{rj}^{mis}, \quad (3)$$

where superscripts *imm* and *mis* represent the immiscible and miscible conditions respectively;  $F_k$  is a factor used to describe the degree of miscibility:

$$F_k = \min \left[ 1, \left( \frac{\sigma}{\sigma_0} \right)^{0.25} \right], \quad (4)$$

$$\sigma^{1/4} = \sum_{c=1}^{n_c} P_{chc} (x_{co} \rho_o - x_{cg} \rho_g), \quad (5)$$

where  $\sigma$  is the surface tension;  $\sigma_0$  is a reference surface tension;  $P_{chc}$  is the parachor of component  $c$ ; subscripts  $o$  and  $g$  represent the oil and gas phases respectively. The relative permeability curve of phase  $j$  under miscible condition is assumed to be a straight line (Li et al., 2016).

The transport equations are discretized in space by the finite volume method and are discretized in time by the backward Euler approximation. Then, the discretized form can be written as follows:

$$\left( V_{gb} \phi \sum_{j=1}^{n_p} x_{cj} \rho_j S_j \right)^{n+1} - \left( V_{gb} \phi \sum_{j=1}^{n_p} x_{cj} \rho_j S_j \right)^n - \Delta t \sum_l \sum_{j=1}^{n_p} \left( x_{cj}^l \lambda_j^l \rho_j^l \gamma^l \Delta P \right) + \Delta t V \sum_{j=1}^{n_p} x_{cj} \rho_j \tilde{q}_j = 0. \quad (6)$$

Where  $V_{gb}$  represents the grid-block volume;  $l$  represents the interfaces of a grid block; the mobility of phase  $j$  over interface  $l$  that is defined as  $\lambda_j^l = (k_{rj}/\mu_j)^l$  is obtained by upstream weighting as well as  $\rho_j^l$ ;  $n+1$  and  $n$  mean the current and previous time steps.

### 2.2. Thermodynamic equilibrium

In EoS based compositional model, the thermodynamic equilibrium is applied to describe the mass transfer of hydrocarbons between oil and gas phases that is the main mechanism and benefit of the CO<sub>2</sub>-EOR technology. For a full representation of the thermodynamic equilibrium,

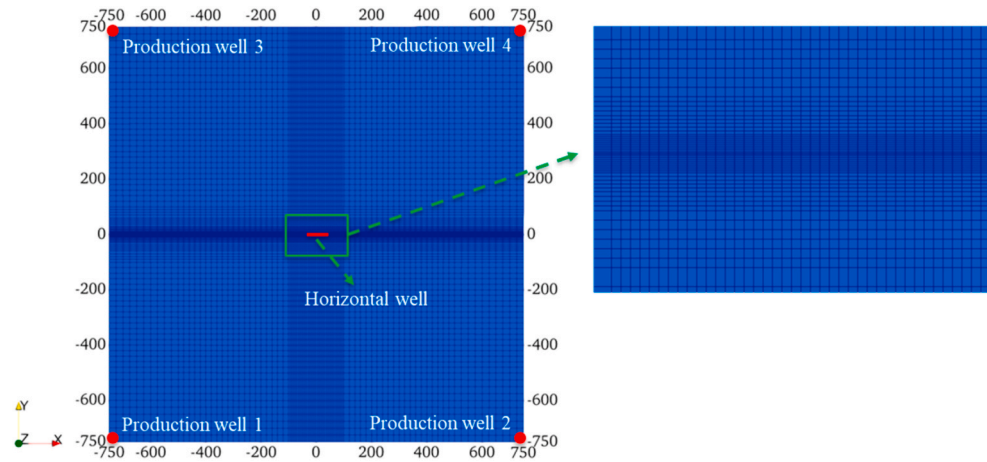


Fig. 1. A high-resolution non-uniform grid used for simulation (321300 cells).

we need to solve a severely nonlinear system that is composed of Eqs. (7)–(10).

$$z_c = Vx_{cg} + Lx_{co}, \quad c = 1, \dots, n_c, \quad (7)$$

$$\varphi_c^L x_{co} = \varphi_c^V x_{cg}, \quad c = 1, \dots, n_c, \quad (8)$$

$$L + V = 1, \quad (9)$$

$$\sum_{c=1}^{n_c} (x_{co} - x_{cg}) = 0. \quad (10)$$

Where  $L$  is the mole fraction of oil phase;  $V$  is the mole fraction of gas phase; subscripts  $o$  and  $g$  represent oil and gas phases;  $z_c$  is the mole fraction of component  $c$  in the hydrocarbon mixture;  $\varphi$  is the fugacity coefficient calculated through Equation of State such as PR and SRK.

With known pressure, temperature, and a hydrocarbon mixture, we can determine the mole fractions of hydrocarbon components in the oil and gas phases by using the multiphase flash. Then, we are able to calculate the parameters such as viscosity, density, saturation, and relative permeability of each phase that are required in the transport equations.

### 2.3. Wellbore storage model

We apply the wellbore storage model to consider the transient flow in well. The model can be described as follows:

$$q - q_b = \rho_i C \frac{\partial P_{wf}}{\partial t}. \quad (11)$$

$$q_b = \sum_{i=1}^{n_{perf}} \left\{ WI_i \sum_{j=1}^{n_p} \sum_{c=1}^{n_c} \left[ x_{cj} \rho_j \frac{k_{rj}}{\mu_j} (P_{wf} - P_i) \right] \right\}. \quad (12)$$

Where  $q$  is the constant molar rate;  $q_b$  is the sandface molar rate;  $\rho_t$  is the molar density of the mixture in the wellbore;  $C$  is the wellbore storage coefficient;  $P_{wf}$  is the bottom hole pressure;  $n_{perf}$  is the number of perforated blocks along the horizontal well;  $P_i$  is the pressure of the  $i$ th perforated block;  $WI$  is the well index which can be shown as follows when the horizontal well is in the  $x$ -direction.

$$WI = \frac{CF \sqrt{K_y K_z} \Delta x}{\ln(r_o/r_w) + s}, \quad (13)$$

where  $CF$  is the conversion factor;  $s$  is the skin factor;  $r_o$  is the equivalent wellbore radius that is derived by Peaceman (1983):

Table 1  
Reservoir parameters.

Parameter	Value	Unit
Reservoir size	1500 × 1500 × 32	m
Initial pressure	80	bar
Temperature	353.15	K
Horizontal permeability	50	mD
Vertical permeability	50	mD
Porosity	0.2	–
Rock compressibility	7.2519e-5	bar <sup>-1</sup>
Reference surface tension	1.0	dynes/cm
Mole fraction (CO <sub>2</sub> , C <sub>4</sub> , C <sub>10</sub> )	0.1, 0.3, 0.6	–

Table 2  
Well parameters.

Well	Well type	Wellbore radius	Skin factor	Wellbore storage coefficient
Injection well	Horizontal	0.1 m	0	0.1 m <sup>3</sup> /bar
Production wells	Vertical	0.1 m	0	0 m <sup>3</sup> /bar

$$r_o = 0.28 \frac{\left[ (K_z/K_y)^{1/2} \Delta y^2 + (K_y/K_z)^{1/2} \Delta z^2 \right]^{1/2}}{(K_z/K_y)^{1/4} + (K_y/K_z)^{1/4}}. \quad (14)$$

### 3. Pressure transient analysis

In this section, we will study the pressure transient behavior of a horizontal well during CO<sub>2</sub> flooding systematically. First, we present a new approach that interprets the complex pressure response curve in two steps to deeply analyze the characteristics of the pressure transient behavior. Next, we conduct a systematic sensitivity analysis with respect to multiple parameters to have a full understanding of the behavior.

Table 3  
Injection/production strategy (The 2nd stage is the shut-in period).

Stage	Simulation time	Injection well (Rate control)	Production wells (BHP control)
1st stage	2000 days	10000 kmol/day	60 bar
2nd stage	1000 h	0 kmol/day	60 bar

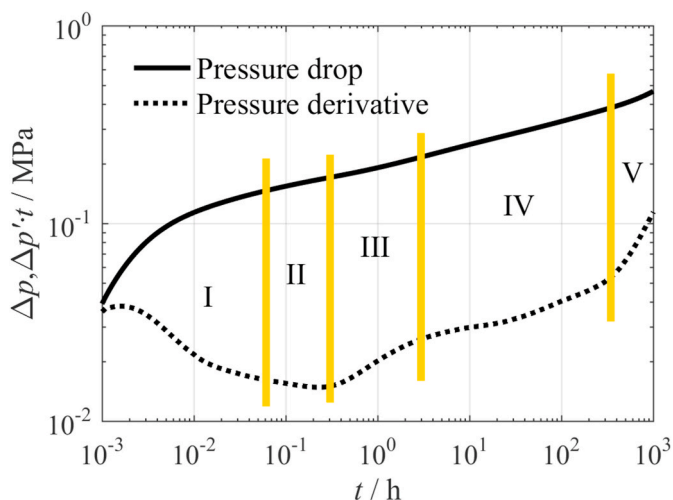


Fig. 2. Log-log plots of pressure change and pressure derivative at an immiscible condition. Five flow regimes are identified.

3.1. Interpretation method of the pressure transient data

Since the pressure transient data measured during the injection period could be noisy, especially for gas injection wells, we will analyze the data that is measured during the shut-in period. To complete a reliable analysis, we run a 3D simulation of CO<sub>2</sub> flooding on a high-resolution non-uniform grid that is shown in Fig. 1. The simulation parameters are listed in Tables 1–3. Four vertical production wells are located at the corners of the reservoir; a horizontal CO<sub>2</sub> injection well along the x-direction is located at the center of the reservoir with a well length equalling 60 m.

We present a new approach to have a basic understanding of the characteristics of the pressure response curve and find the root cause of the particular transient behaviors. To reach this goal, we interpret the curve in two steps. First, we identify the typical flow regimes of horizontal wells with the traditional pressure transient analysis method. Second, we analyze the effect of the component banks that are induced by the complex mechanisms of CO<sub>2</sub> flooding on the type curves through the corresponding analysis method (Li et al., 2018).

3.1.1. Identification of typical flow regimes

Here, we interpret the pressure transient data with a traditional theory where a combined log-log plot of pressure and pressure derivative is taken as a diagnostic and interpretation tool. As shown in Fig. 2, we identify five flow regimes with different durations.

**Regime I: afterflow.** The flow in this period is mainly controlled by the compressibility of the fluid in the wellbore and the skin factor. Thus, the data in this period contains little or no information related to the reservoir.

**Regime II: early-time radial flow.** The flow pattern in this period is radial around the wellbore. Usually, it continues until the effect of the upper and lower boundary is felt at the wellbore.

**Regime III: intermediate-time linear flow.** If the well length is much longer than the formation thickness, this linear flow may occur after the effect of the two impermeable boundaries in vertical direction is felt at the wellbore.

**Regime IV: pseudo-late radial flow.** If the reservoir domain is large enough, this flow regime will take place when the intermediate-time linear flow regime is finished but the pressure transient does not reach the outer boundaries yet. Usually, the pressure derivative flattens in this period. But the complex mechanisms of CO<sub>2</sub> flooding that induce a nonuniform mobility distribution make the transient behavior of this regime different. We will interpret the characteristics of the curves in detail in the next section.

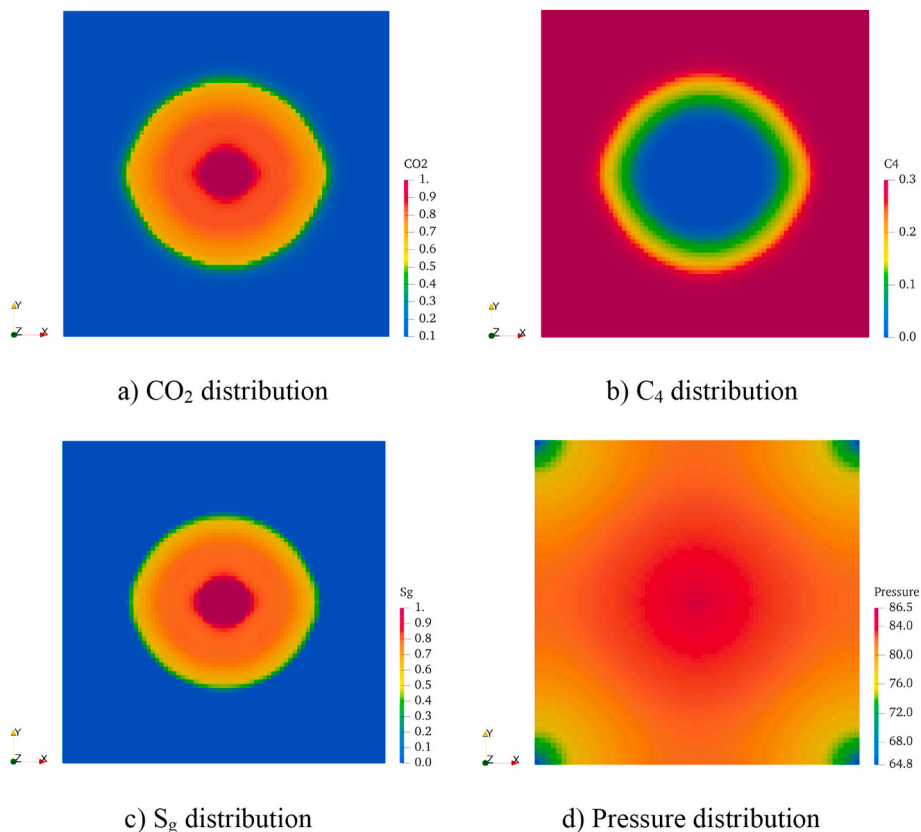


Fig. 3. CO<sub>2</sub>, C<sub>4</sub>, S<sub>g</sub>, and pressure distributions at an immiscible condition (T = 2000 days).

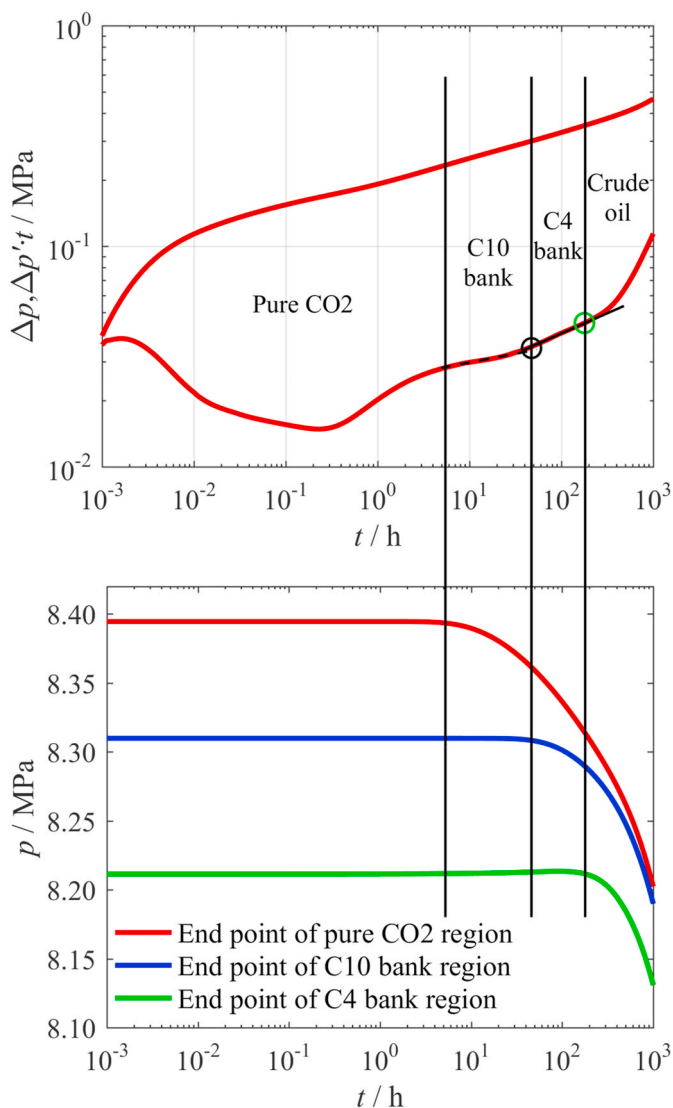


Fig. 4. Interpret the pressure response curve with the corresponding analysis method (at an immiscible condition). The centroids of the grid blocks that are taken as the end points of pure CO<sub>2</sub> region, C<sub>10</sub> bank, and C<sub>4</sub> bank are [72.5, 85], [150, 230], and [230, 410] respectively.

**Regime V: boundary dominated flow.** In the late time of the test, we will observe a boundary dominated flow once the pressure transient reaches the outer boundary.

### 3.1.2. The effect of complex mechanisms of CO<sub>2</sub> flooding

The distributions of CO<sub>2</sub>, C<sub>4</sub>, S<sub>g</sub>, and pressure are shown in Fig. 3 from where we can see that the injected CO<sub>2</sub> displaces the crude oil at an immiscible condition. Moreover, we find several distinguishable regions such as pure CO<sub>2</sub> region, C<sub>10</sub> bank where there is no C<sub>4</sub> and is not filled with pure CO<sub>2</sub>, C<sub>4</sub> bank, and crude oil region. As the phase behaviors in the regions differ a lot, the effect of the four regions should be taken into account for the pressure transient analysis if we want to know the root causes of the particular transient behaviors. We will investigate how these component banks affect the curves through the corresponding analysis method (Li et al., 2018).

In Fig. 4, we draw the pressure variations of three grid blocks which are located at the outer boundaries of the pure CO<sub>2</sub> region, C<sub>10</sub> bank, and C<sub>4</sub> bank. By aligning the x-coordinate with the log-log plot of pressure and pressure derivative, we are able to determine the time when the effects of C<sub>10</sub> bank, C<sub>4</sub> bank, and crude oil region are felt at the wellbore.

Then, we figure out four durations on the curves that correspond to the component banks and get new insights into the pressure transient behavior.

**Pure CO<sub>2</sub> region.** The early-time radial flow and intermediate-time linear flow are both developed inside the pure CO<sub>2</sub> region. Since the component distribution in this region is uniform, the characteristics of the pressure derivative curve are similar to that from traditional models assuming a horizontal well in a single-phase reservoir.

**C<sub>10</sub> bank.** The effect of this bank is felt at the wellbore in the pseudo-late radial flow regime. Usually, the pressure derivative curve in this regime is flat according to the theories of traditional models. However, in CO<sub>2</sub>-EOR, the existence of the C<sub>10</sub> bank which holds lower mobility than that of the pure CO<sub>2</sub> region changes the behavior of this flow regime and makes the derivative go up.

**C<sub>4</sub> bank.** The pseudo-late radial flow continues in the C<sub>4</sub> bank. Controlled by the complex mechanisms of CO<sub>2</sub> flooding, the C<sub>4</sub> starts to emerge and leads to a sharp reduction in gas saturation in this region. It results in a reduction of the mobility which affects the characteristics of the curves and makes the pressure derivative move upward with a higher positive slope.

**Crude oil region.** The pseudo-late radial flow continues in the crude oil region as well. Without any injected CO<sub>2</sub>, the mobility in this region is even lower than the C<sub>4</sub> bank which makes the pressure derivative curve go up furthermore. Providing enough shut-in duration, the boundary dominated flow regime could also occur in this region once the pressure transient reaches the outer boundary.

## 3.2. Systematic analysis of the pressure transient data

In this section, we will conduct a systematic analysis of the pressure transient data by studying the sensitivity of the curves to multiple parameters such as miscible condition, wellbore storage coefficient, skin factor, horizontal well length, anisotropy, and amount of injected CO<sub>2</sub>.

### 3.2.1. Miscibility

The development of miscibility makes the leading and trailing shocks closer and changes the component banks. Thus, the miscibility will have an influence on the pressure transient behavior. Here, we change the initial pressure to 170 bar and the bottom hole pressure of producers to 150 bar. From the distributions of CO<sub>2</sub>, C<sub>4</sub>, S<sub>g</sub>, and pressure in Fig. 5, we can see that the flooding process is under a miscible condition. Then, we could compare the curves at the miscible condition to those at the immiscible condition. Note, the settings in this case are applied in the following cases as well.

The curves at miscible and immiscible conditions are shown in Fig. 6. It is clear that miscibility has a great influence on the pressure transient behavior. The pressure and pressure derivative curves at the miscible condition are lower than those at the immiscible condition. What is important is that it turns out a typical pseudo-late radial flow regime. To quantitatively interpret the difference, we will analyze the effect of component banks on the curves using the corresponding analysis method again.

From Fig. 7, we can see that the duration corresponding to the pure CO<sub>2</sub> region is much longer than that at the immiscible condition. As there is time enough to develop a pseudo-late radial flow regime, we can observe a nearly horizontal line in the pure CO<sub>2</sub> region which is similar to the traditional horizontal well test models. Besides, the durations corresponding to the C<sub>10</sub> and C<sub>4</sub> banks are significantly shrunk. The reason is that with the development of the miscibility, the leading shock and trailing shock become very sharp and approach each other. It results in a drastically shrunk mixing zone which further reduces the corresponding time duration on the curves. Moreover, the fact that the difference of fluid properties between pure CO<sub>2</sub>, C<sub>4</sub>, and C<sub>10</sub> banks is much less than that at the immiscible condition mitigates the upward trend of the pressure derivative curve. It points out a promising approach to estimate the miscibility underground from the difference of the curves

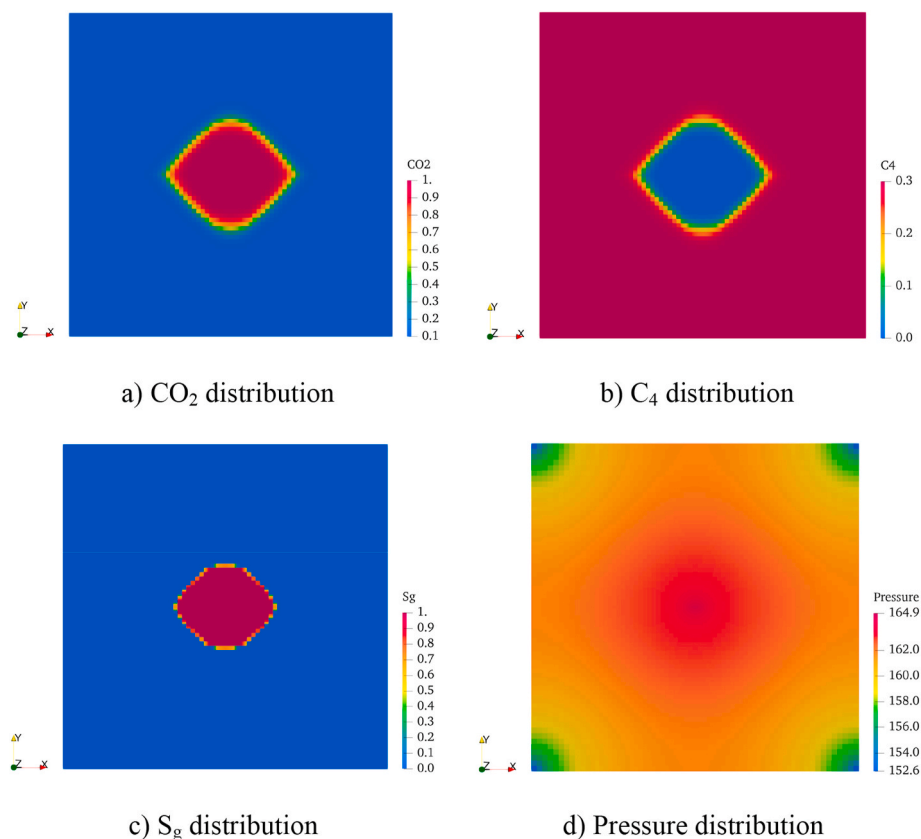


Fig. 5. CO<sub>2</sub>, C<sub>4</sub>, S<sub>g</sub>, and pressure distributions at a miscible condition (T = 2000 days).

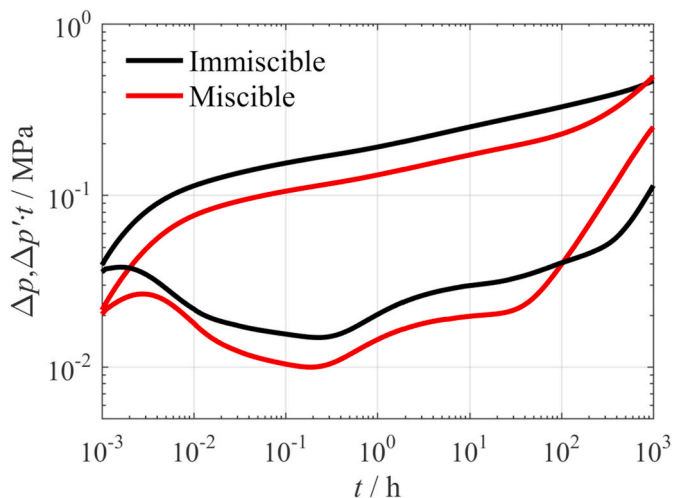


Fig. 6. The effect of miscibility on the pressure and pressure derivative curves.

between miscible and immiscible conditions.

### 3.2.2. Wellbore storage coefficient

The injection well may have a large wellbore storage coefficient owing to the high compressibility of pure CO<sub>2</sub>. We should know how the coefficient influences the pressure transient behavior in a wide range to design a proper location of the packer. For this purpose, we run several simulations with different wellbore storage coefficients. As shown in Fig. 8, the coefficient has a great influence on the curves, especially in the early time flow regimes. The developing time of the regimes is postponed and even covered with its increase. What is worse, a

significantly high coefficient, which could be introduced by a long horizontal well, will not only cover the behaviors of early-time flow regimes but also the intermediate-time linear flow and even the pseudo-steady radial flow. As a result, to make the pressure transient data reflect more information in the reservoir, the downhole shut-in tool that can minimize the wellbore storage effect is highly recommended for the well test of a horizontal CO<sub>2</sub> injection well.

### 3.2.3. Skin factor

The skin factor is an important parameter to characterize the well condition. Here, we will run several simulations with different skin factors to investigate their effect on the pressure transient behavior. From Fig. 9, we can find that the curves are sensitive to the skin factor. The pressure drop curve goes up with the increase of the skin factor when the derivative curve only moves upward in the early time flow regimes. It points out a promising prospect that the permeability modification, which is caused by CO<sub>2</sub>-fluid-rock interactions and is a concern in the CO<sub>2</sub> injectivity analysis, can be estimated by making use of the pressure transient data.

### 3.2.4. Horizontal well length

It is quite important for a field manager to know the well length that has a great influence on the CO<sub>2</sub>-EOR performance before making any decisions. However, the fact that the effective length is often less than the drilled length makes it difficult. As an effective way, the pressure transient data is usually applied to evaluate the effective length according to the traditional horizontal well test models. In this work, we should investigate whether the component banks induced by the complex mechanisms of CO<sub>2</sub> flooding degenerate it or not.

We run simulations with the well length equalling 30, 60, 90 m respectively. From Fig. 10, we can see that the length has a great influence on the curves. The pressure drop curve moves downward with the increase of the length when the pressure derivative curve only moves

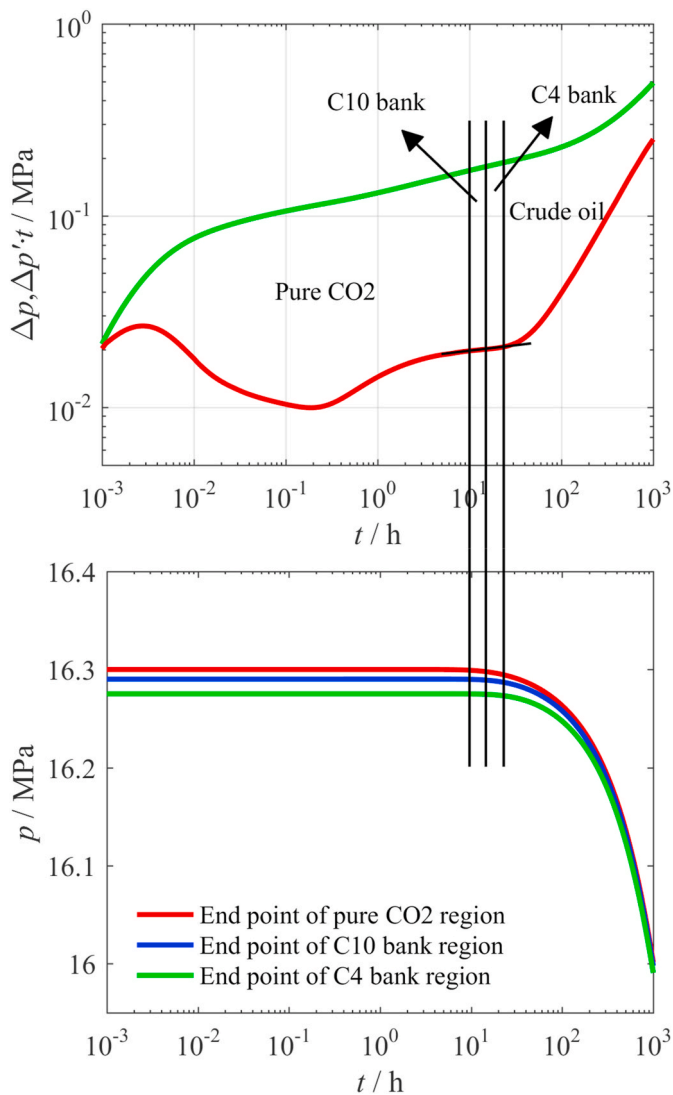


Fig. 7. Interpret the pressure response curve with the corresponding analysis method (at a miscible condition). The centroids of the grid blocks that are taken as the end points of pure CO<sub>2</sub> region, C<sub>10</sub> bank, and C<sub>4</sub> bank are [110, 130], [130, 170], and [150, 210] respectively.

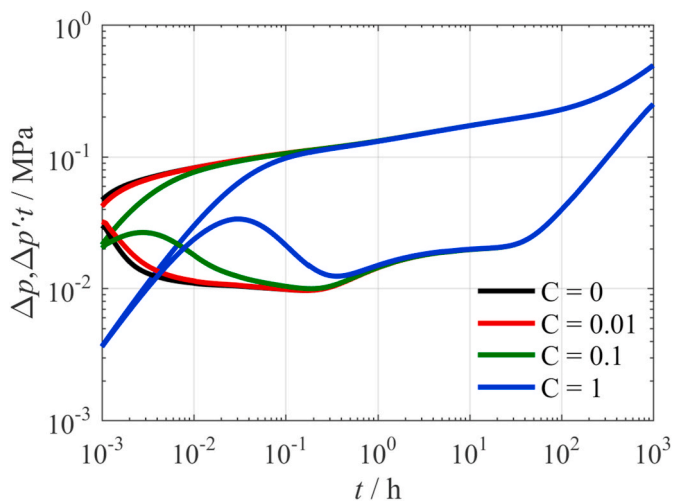


Fig. 8. The effect of wellbore storage coefficient on the pressure and pressure derivative curves.

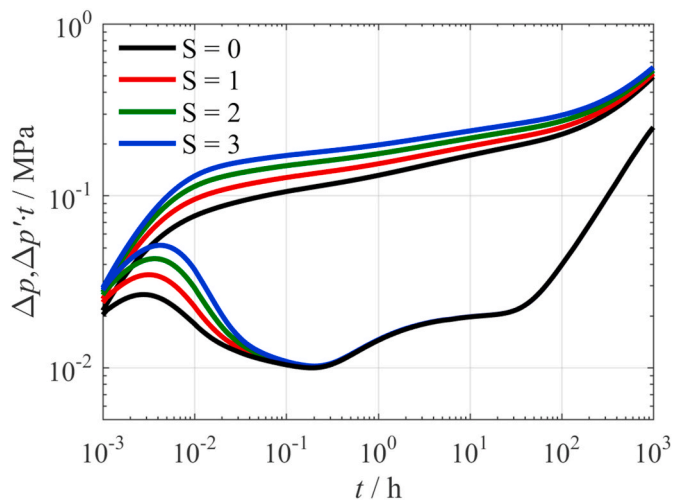


Fig. 9. The effect of skin factor on the pressure and pressure derivative curves.

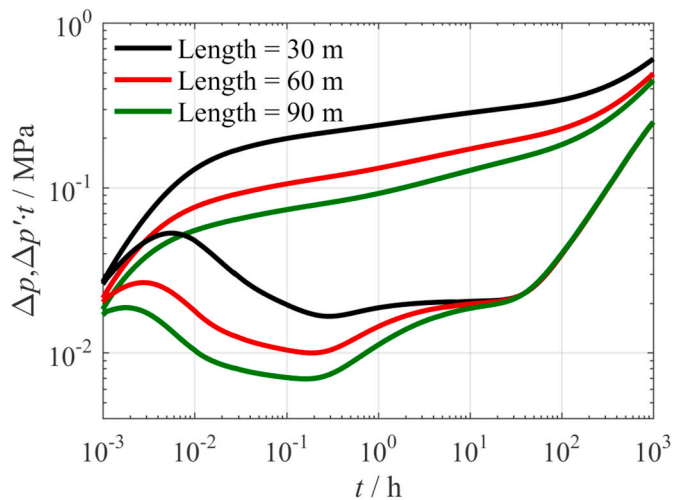


Fig. 10. The effect of well length on the pressure and pressure derivative curves.

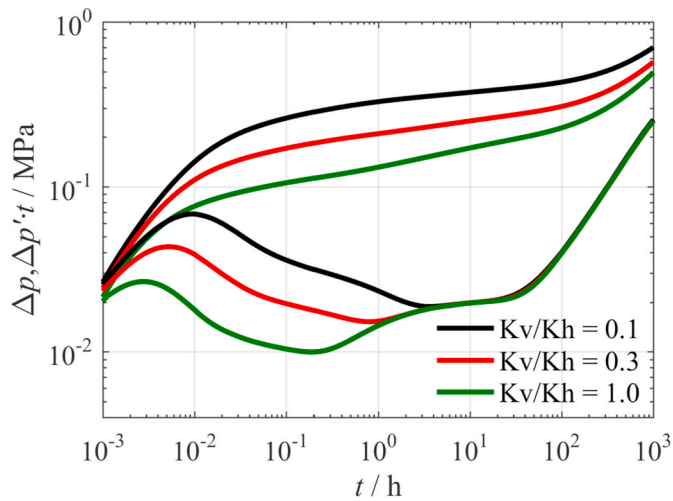


Fig. 11. The effect of anisotropy on the pressure and pressure derivative curves.

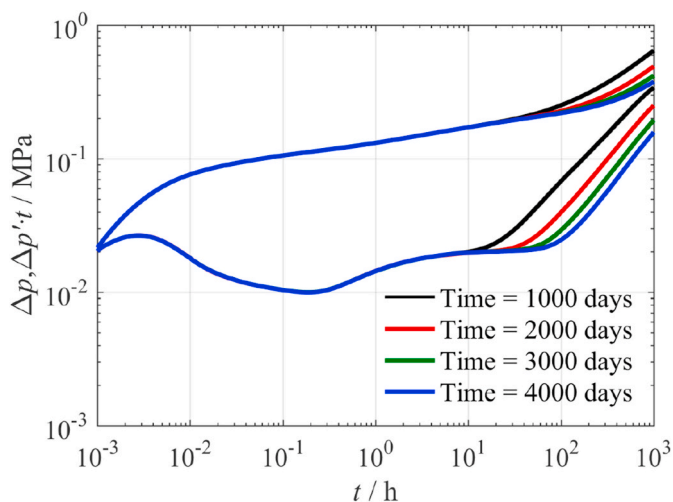


Fig. 12. The effect of injection time (amount of injected CO<sub>2</sub>) on the pressure and pressure derivative curves.

downward before a certain time. The reason is that a longer horizontal well that connects the well and formation better reduces the flow resistance. Thanks to the sensitivity, we feel confident to apply the pressure transient data to evaluate the effective length during CO<sub>2</sub> flooding.

### 3.2.5. Ratio of vertical to horizontal permeability

Another important factor affecting the CO<sub>2</sub>-EOR performance is the anisotropy. Here, we run several simulations with different ratios of vertical to horizontal permeability. As we can see in Fig. 11, the ratio influences the curves significantly. The pressure drop curve moves downward with its increase when the pressure derivative curve goes down before the pseudo-late radial flow regime. Moreover, it becomes difficult to identify the first radial flow regime on the pressure derivative curve when the ratio is small. In other words, the first radial flow regime may fail to develop in severe anisotropy cases. Benefit from the sensitivity, we could apply the pressure transient data to estimate the anisotropy underground as well.

### 3.2.6. Amount of injected CO<sub>2</sub>

Continuous monitoring of the CO<sub>2</sub> displacement process based on well test holds promising prospects since the measurement of the bottom hole pressure is cheap and easy to operate. But the feasibility of this approach is dependent on the sensitivity of the curves to the amount of injected CO<sub>2</sub>. In this work, we run several simulations with different injection time. From Fig. 12, we can find that the amount of injected CO<sub>2</sub> has a great effect on the curves. The time when the crude oil region is felt at the wellbore is postponed with the increase of the amount of injected CO<sub>2</sub>. The reason is that the high compressibility of the CO<sub>2</sub> could slow down the propagation of the transient pressure. Therefore, we can conclude that the pressure transient data is sensitive to the amount of injected CO<sub>2</sub> and can be used to continuously monitor the CO<sub>2</sub> displacement process.

## 4. Conclusions

In this work, we have coupled the wellbore storage model and EoS based compositional model in a fully-implicit parallel reservoir simulator. The two models enable the simulator to reproduce the transient flow in well and the complex displacement process during CO<sub>2</sub>-EOR respectively. The CPU-based parallel algorithm makes it possible to run a simulation on a high-resolution non-uniform grid that helps to capture the transient behaviors during CO<sub>2</sub> flooding accurately.

We presented a new approach that interprets the pressure response

curve in two steps. First, we identified five flow regimes on the type curves according to the traditional pressure transient analysis method for horizontal wells. Based on that, we get a basic understanding of the flow patterns as well as the characteristics of the pressure transient behavior. Second, we interpreted the type curves furthermore through the corresponding analysis method. We figured out the durations on the curves that correspond to different component banks. Then, we conducted a root cause analysis in detail for the particular transient behaviors by taking the phase behavior of each bank into the interpretation. After all, we have a deep understanding of the pressure transient behavior of a horizontal well during CO<sub>2</sub>-EOR.

Besides, we investigated the sensitivity of the pressure transient data to the miscible condition, wellbore storage coefficient, skin factor, horizontal well length, anisotropy, and amount of injected CO<sub>2</sub>. The systematic sensitivity analysis points out that the multiple parameters both have an influence on the data. Meanwhile, the way these parameters act on the type curves indicates the feasibility of applying the measured transient data for parameter evaluation. We can conclude that the work in this paper provides a cheap and reliable way to monitor the CO<sub>2</sub> displacement process in horizontal well patterns.

The water alternating gas (WAG) injection could improve the sweep efficiency of CO<sub>2</sub>-EOR. But inappropriately designed WAG parameters will reduce the performance significantly. We will investigate the feasibility of monitoring the more complicated displacement process with pressure transient data. Moreover, we want to point out that the CCS process where CO<sub>2</sub> is injected into saline aquifers is similar to the immiscible flooding process in this work. However, since the properties of saline water and hydrocarbon may differ a lot, we need to invest more effort in the multiphase transient analysis during saline aquifer CO<sub>2</sub> storage. Besides, we will investigate the effect of capillary pressure on the pressure transient behavior during CO<sub>2</sub>-EOR in our future work.

## Author statement

Longlong Li: Conceptualization, Methodology, Software, Investigation, Writing – original draft, Writing – review & editing, Minglu Wu: Methodology, Investigation, Writing – review & editing, Yuewu Liu: Investigation, Writing – review & editing, Jiuge Ding: Investigation, Writing – review & editing, Ahmad Abushaikha: Writing – original draft, Funding acquisition

## Declaration of competing interest

The authors declare that they have no known competing financial interests or personal relationships that could have appeared to influence the work reported in this paper.

## Acknowledgment

This publication was supported by the National Priorities Research Program grant NPRP10-0208-170407 from Qatar National Research Fund.

## References

- Altundas, B., Chugunov, N., Ramakrishnan, T.S., et al., 2017. Quantifying the Effect of CO<sub>2</sub> Dissolution on Seismic Monitoring of CO<sub>2</sub> in CO<sub>2</sub>-EOR, 2017. SEG International Exposition and Annual Meeting, Houston, Texas.
- Araman, A.W., Hoffman, M., Davis, T.L., 2008. Thief zone identification through seismic monitoring of a CO<sub>2</sub> flood, weyburn field, saskatchewan. In: 2008 SEG Annual Meeting. Society of Exploration Geophysicists, Las Vegas, Nevada.
- Bagci, A.S., 2007. Immiscible CO<sub>2</sub> flooding through horizontal wells. *Energy Sources A* 29, 85–95.
- Cheng, Y., 2003. Pressure Transient Testing and Productivity Analysis for Horizontal Wells. Texas A&M University.
- Choi, J., Nicot, J., Hosseini, S.A., et al., 2013. CO<sub>2</sub> recycling accounting and EOR operation scheduling to assist in storage capacity assessment at a U.S. gulf coast depleted reservoir. *Int. J. Greenh. Gas Con.* 18, 474–484.



- Clonts, M.D., Ramey, H.J., 1986. Pressure Transient Analysis for Wells with Horizontal Drainholes. SPE California Regional Meeting, Oakland, California. SPE-15116-MS.
- Daviau, F., Mouronval, G., Bourdarot, G., et al., 1988. Pressure analysis for horizontal wells. SPE form. Evaluation 3, 716–724.
- Ghahfarokhi, R.B., Pennell, S., Matson, M., et al., 2016. Overview of CO<sub>2</sub> Injection and WAG Sensitivity in SACROC. SPE Improved Oil Recovery Conference, Tulsa, Oklahoma, USA.
- Goode, P.A., Thambynayagam, R.M., 1987. Pressure drawdown and buildup analysis of horizontal wells in anisotropic media. SPE Form. Eval. 2, 683–697.
- Hosseinoosheri, P., Hosseini, S.A., Nuñez-López, V., et al., 2018. Impact of field development strategies on CO<sub>2</sub> trapping mechanisms in a CO<sub>2</sub>-EOR field: a case study in the permian basin (SACROC unit). Int. J. Greenh. Gas Con. 72, 92–104.
- Kendall, R.R., Winarsky, R., Davis, T.L., et al., 2003. 9C, 4D seismic processing for the weyburn CO<sub>2</sub> flood, saskatchewan, Canada. In: SEG Annual Meeting. Society of Exploration Geophysicists, Dallas, Texas.
- Kuchuk, F.J., 1995. Well testing and interpretation for horizontal wells. J. Petrol. Technol. 47, 36–41.
- Kuchuk, F.J., Goode, P.A., Wilkinson, D.J., et al., 1991. Pressure-transient behavior of horizontal wells with and without gas cap or aquifer. SPE Form. Eval. 6, 86–94.
- Li, L., Abushaikh, A., 2019. Development of an advancing parallel framework for reservoir simulation. In: Third EAGE WIPIC Workshop: Reservoir Management in Carbonates. Doha, Qatar.
- Li, L., Abushaikh, A., 2020. An advanced parallel framework for reservoir simulation with mimetic finite difference discretization and operator-based linearization. In: ECMOR XVII-17th European Conference on the Mathematics of Oil Recovery.
- Li, L., Abushaikh, A., 2021. A fully-implicit parallel framework for complex reservoir simulation with mimetic finite difference discretization and operator-based linearization. Comput. Geosci.
- Li, L., Yao, J., Li, Y., et al., 2016. Pressure-transient analysis of CO<sub>2</sub> flooding based on a compositional method. J. Nat. Gas Sci. Eng. 33, 30–36.
- Li, L., Voskov, D.V., Yao, J., et al., 2018. Multiphase transient analysis for monitoring of CO<sub>2</sub> flooding. J. Petrol. Sci. Eng. 160, 537–554.
- Li, L., Khait, M., Voskov, D.V., Abushaikh, A., 2020. Parallel framework for complex reservoir simulation with advanced discretization and linearization schemes. In: SPE Europec Featured at 82nd EAGE Conference and Exhibition. SPE-200615-MS, Amsterdam, Netherlands.
- Lohrenz, J., Bray, B.G., Clark, C.R., 1964. Calculating viscosities of reservoir fluids from their compositions. J. Petrol. Technol. 16 (10), 1171–1176.
- Lyu, X., Voskov, D., Rossen, W.R., 2021. Numerical investigations of foam-assisted CO<sub>2</sub> storage in saline aquifers. Int. J. Greenh. Gas Con. 108, 103314.
- MacAllister, D.J., 1987. Pressure transient analysis of CO<sub>2</sub> and enriched-gas injection and production wells. In: SPE Annual Technical Conference and Exhibition. Society of Petroleum Engineers Source, San Antonio, Texas.
- Malik, Q.M., Islam, M.R., 2000. CO<sub>2</sub> Injection in the Weyburn Field of Canada: Optimization of Enhanced Oil Recovery and Greenhouse Gas Storage with Horizontal Wells. SPE/DOE improved oil recovery symposium.
- Massarweh, O., Abushaikh, A., 2021. A review of recent developments in CO<sub>2</sub> mobility control in enhanced oil recovery. Petroleum.
- Moortgat, J., 2016. Viscous and gravitational fingering in multiphase compositional and compressible flow. Adv. Water Resour. 89, 53–66.
- Nordhaus, W.D., 1991. To slow or not to slow: the economics of the greenhouse effect. Econ. J. 101 (407), 920–937.
- Odeh, A.S., Babu, D.K., 1989. Transient Flow Behavior of Horizontal Wells, Pressure Drawdown, and Buildup Analysis. SPE California Regional Meeting, Bakersfield, California.
- Orr Jr., F.M., Taber, J.J., 1984. Use of carbon dioxide in enhanced oil recovery. Science 224, 563–570.
- Ozkan, E., Raghavan, R., Joshi, S.D., 1989. Horizontal well pressure analysis. SPE form. Evaluation 4, 567–575.
- Peaceman, D.W., 1983. Interpretation of well-block pressures in numerical reservoir simulation with nonsquare grid blocks and anisotropic permeability. SPE J. 23 (3), 531–543.
- Rognmo, A.U., Fredriksen, S.B., Alcorn, Z.P., et al., 2019. Pore-to-Core EOR upscaling for CO<sub>2</sub> foam for CCUS. SPE J. 24, 2793–2803.
- Rognmo, A.U., Al-Khayyat, N., Heldal, S., et al., 2020. Performance of silica nanoparticles in CO<sub>2</sub> foam for EOR and CCUS at tough reservoir conditions. SPE J. 25, 406–415.
- Rosa, A.J., Carvalho, R. de S., 1989. A mathematical model for pressure evaluation in an infinite-conductivity horizontal well. SPE form. Evaluation 4, 559–566.
- Schneider, S.H., 1989. The greenhouse effect: science and policy. Science 243 (4892), 771–781.
- Su, K., Liao, X.W., Zhao, X.L., 2015. Transient pressure analysis and interpretation for analytical composite model of CO<sub>2</sub> flooding. J. Petrol. Sci. Eng. 125, 128–135.
- Sun, H., Yao, J., Gao, S., et al., 2013. Numerical study of CO<sub>2</sub> enhanced natural gas recovery and sequestration in shale gas reservoirs. Int. J. Greenh. Gas Con. 19, 406–419.
- Tang, R.W., Ambastha, A.K., 1988. Analysis of CO<sub>2</sub> pressure transient data with two-and three-region analytical radial composite models. In: SPE Annual Technical Conference and Exhibition. Society of Petroleum Engineers, Houston, Texas.
- Tchelepi, H.A., Orr Jr., F.M., Rakotomalala, N., et al., 1993. Dispersion, permeability heterogeneity, and viscous fingering: acoustic experimental observations and particle-tracking simulations. Phys. Fluids 5 (7), 1558–1574.
- Terrell, M.J., Davis, T.L., Brown, L., et al., 2002. Seismic monitoring of a CO<sub>2</sub> flood at weyburn field, saskatchewan, Canada: demonstrating the robustness of time-lapse seismology. In: 2002 SEG Annual Meeting. Society of Exploration Geophysicists, Salt Lake City, Utah.
- Tian, S., Zhao, G., 2008. Monitoring and predicting CO<sub>2</sub> flooding using material balance equations. J. Can. Pet. Technol. 47 (11), 41–47.
- Wang, S., Di, Y., Winterfeld, P.H., et al., 2021. Understanding the multiphysical processes in carbon dioxide enhanced-oil-recovery operations: a numerical study using a general simulation framework. SPE J. 26, 918–939.
- Yao, J., Wu, M., 2011. Streamline Numerical Well Test Interpretation. Gulf Professional Publishing.
- Zhang, L., Ren, B., Huang, H., et al., 2015. CO<sub>2</sub> EOR and storage in Jilin oilfield China: monitoring program and preliminary results. J. Petrol. Sci. Eng. 125, 1–12.